Available online at www.sciencedirect.com
SCIENCE DIRECT®
International Journal of Thermal Sciences 45 (2006) 729–737
International Journal of Thermal Sciences
www.elsevier.com/locate/ijts

Thermodynamic analysis of optimal curvature ratio for fully developed laminar forced convection in a helical coiled tube with uniform heat flux

T.H. Ko *

Department of Mechanical Engineering, Lunghwa University of Science and Technology, 300, Wan-Shou Rd. Sec. 1, Kueishan, 33306 Taoyuan, Taiwan, ROC

Received 17 January 2005; received in revised form 10 August 2005; accepted 10 August 2005

Available online 19 September 2005

Abstract

In the present paper, the optimal curvature ratio for steady, laminar, fully developed forced convection in a helical coiled tube with constant wall heat flux was analyzed by thermodynamic second law based on minimal entropy generation principle. Two working fluids, including air and water, are considered. The entropy generation analysis covers a Reynolds number (*Re*) range of 100 to 10 000, a coil curvature ratio (δ) range of 0.01 to 0.3, and two dimensionless duty parameters related with fluid properties, wall heat flux and mass flow rate, η_1 range of 0.1 to 3.0, and $\eta_2/10^{20}$ range of 0.01 to 1.0. The optimal δ for cases with various combinations of the design parameters is given in the present paper. In addition, a correlation equation for the optimal δ as a function of *Re*, η_1 and η_2 is proposed through a least-square-error analysis. For a thermal system composed of helical coiled tubes with fixed *Re*, wall heat flux and mass flow rate, the optimal δ should be selected so that the system could have the best exergy utilization and least irreversibility.

Keywords: Thermodynamic second law; Minimal entropy generation principle; Exergy; Irreversibility; Helical coiled tube

1. Introduction

Laminar convective heat transfer in helical coiled tubes is commonly encountered in the design of compact heat exchangers, evaporators and condensers used in many industrial applications. Because of the practical importance, a number of theoretical and numerical studies have been presented for investigating the flow fields in the helical coiled tubes. Since the heat transfer performance and pressure drop in helical coiled tubes are two major concerns for practical applications, most of previous studies aimed to clarify the correlations between the friction factor and the Nusselt number [1–4]. Besides, from the review work of Berger et al. [5] and Shah and Joshi [6] on the abundant researches relevant to the fluid flow and heat transfer in helical coiled tubes, it can be seen that the effect of secondary flow motion generated by the curvature effect and centrifugal force in helical coils on pressure drop and heat transfer is a principal focus continuously attracting many researches during the past several decades. In the numerical study of Lin et al. [7] on the laminar forced convection in helical coiled tubes, both Nusselt number and friction factor were found to become large as the curvature ratio (ratio of tube radius to the curvature radius of coiled tube) of the helical coiled tubes increases.

As a good heat-exchanger passage, it is expected that the helical coiled tubes could provide the most effective heat transfer performance and the least pressure drop so that the available energy can be utilized efficiently. However, as other heat exchangers, an inevitable problem met by helical coiled tubes is that the heat transfer enhancement in the flow fields is always achieved at the expense of an increase in friction loss. For example, the heat transfer enhancement method by using alternating axis coils to induce chaotic mixing proposed by Narasimha et al. [8], not only increases the heat transfer rate, but also increases significant pressure drop simultaneously. Such conflict raises the question as to what is the optimal trade-off by selecting the most appropriate geometry and the best flow condition. Recently, the design-related concept of efficient exergy use [9] has become the answer to the question. Based on the minimal entropy generation principle [9], the best exergy utilization and least irreversibility could be obtained in a thermal system

* Tel.: +886 2 82093211; fax: +886 2 82091475.
E-mail address: thko@mail.lhu.edu.tw (T.H. Ko).

1290-0729/$ – see front matter
doi:10.1016/j.ijthermalsci.2005.08.007

Nomenclature

a	radius of coil curvature ..... m	P	pressure ..... Pa
b	coil pitch ..... m	q'	heat transfer rate per unit coil length ..... $W\cdot m^{-1}$
Dn	Dean number, $= Re(r_0/a)^{1/2}$	Re	Reynolds number, $= \rho V(2r_0)/\mu$
f	friction factor	r_0	radius of coil tube ..... m
He	Helical number, $= Dn/[1+(b/2\pi a)^2]^{1/2}$	s	specific entropy generation ..... $J\cdot kg^{-1}\cdot K^{-1}$
h	specific enthalpy ..... $J\cdot kg^{-1}$	$\dot{S}'_{gen}$	entropy generation rate per unit length ..... $W\cdot m^{-1}\cdot K^{-1}$
$\bar{h}$	average heat transfer coefficient in the coil tube ..... $W\cdot m^{-2}\cdot K^{-1}$	T	bulk temperature of the stream ..... K
k	thermal conductivity ..... $W\cdot m^{-1}\cdot K^{-1}$	V	average velocity in the coil tube ..... $m\cdot s^{-1}$
m	exponent in Eq. (12)	*Greek symbols*	
$\dot{m}$	mass flow rate ..... $kg\cdot s^{-1}$	ν	specific volume ..... $m^3\cdot kg^{-1}$
N_S	entropy generation number	η_1	dimensionless parameter, $= \pi kT/q'$
$(N_S)_P$	entropy generation number due to frictional irreversibility	η_2	dimensionless parameter, $= 32\dot{m}^2\rho^2 q'/\mu^5\pi^3$
$(N_S)_T$	entropy generation number due to heat transfer irreversibility	δ	coil-to-tube radius ratio, r_0/a
Nu	Nusselt number, $= \bar{h}(2r_0)/k$	λ	nondimensionless pitch, $b/2\pi a$
		ρ	density ..... $kg\cdot m^{-3}$

while the entropy generation in the system is minimized. Bejan [10] has proposed a systematic methodology of computing entropy generation through heat and fluid flow in heat exchangers, based on which considerable optimal designs of thermal systems have been proposed [11–14]. During the design work of helical coiled tubes, there can be found several important parameters having effective influence on heat and momentum transport phenomena in the devices. Meantime, these parameters also contribute to irreversibility that inherently competes with one another. To find out the optimal trade-off between these design parameters from the view point of best exergy utilization should be worthwhile for developing a thermal system. Nonetheless, in previous investigations relevant to the flow field in helical coiled tubes, most of them were restricted to the first law of thermodynamics. Very rare exergy analysis has been addressed. In a recent work of Ko and Ting [15], an analytical thermodynamic analysis has been carried out for the fully developed laminar forced convection in a helical coiled tube. From the study, it was found that the entropy generation in helical coiled tubes is closely related to the Reynolds number and curvature ratio of coiled tubes, but relatively insensitive to the coiled tube pitch. Based on minimal entropy generation principle, the optimal Reynolds number and curvature ratio of helical coiled tubes were analyzed. However, in the study only some specific flow conditions with particular values of wall heat flux and mass flow rate were considered. In view that the optimal design to induce the minimal entropy generation is closely related with various flow conditions, Ko and Ting [16] extended the research to consider more general flow configurations and wall conditions of the fully developed laminar forced convection in helical coiled tubes. The major concern of the study is the optimal *Re* for the flow fields. Through calculations of multi-dimensional mapping cases, a general correlation equation for the optimal *Re* was successfully derived in the study, based on which the optimal *Re* can be determined according to the realistic flow conditions. As we know the curvature ratio of helical coiled tubes, which has substantial influences on the heat transfer performance and fluid friction in coiled tubes, is another important design parameter in practical applications. Although the analysis of optimal curvature ratio has been carried out in the previous study [15], however, only the resultant entropy generation was analyzed, whereas the independent influences of curvature ratio on entropy generation from frictional and heat transfer irreversibilities were not mentioned. Moreover, as a preliminary study the research only focused on some specific flow conditions. For helical coiled tubes under general flow conditions, there is still lack of thermodynamic analysis about the effects of curvature ratio on entropy generation and the further optimal analysis. In view of this, the present paper intends to investigate the optimal curvature ratio of helical coiled tubes through thermodynamic second law based on the minimal entropy generation principle. The influences of curvature ratio on entropy generation from frictional and heat transfer irreversibility as well as the resultant entropy generation will be analyzed separately in detail. The results of the optimal curvature ratio according to different flow conditions will be given through graphical form. Besides, the correlation equation for providing the optimal curvature ratio as a function of the relevant design parameters to yield the best exergy utilization with minimal entropy generation and the least irreversibility will be proposed.

2. Geometry and parameters of helical coils

Fig. 1 shows a typical helical coiled tube. The principal geometric dimensions include the inner radius of the tube (r_0), the curvature radius of the coil (a) and the coil pitch (increase of height per rotation, b). The curvature ratio, δ, is defined as the tube-to-coil radius ratio, r_0/a. The dimensionless pitch, λ, is defined as $b/2\pi a$. There are four important dimensionless

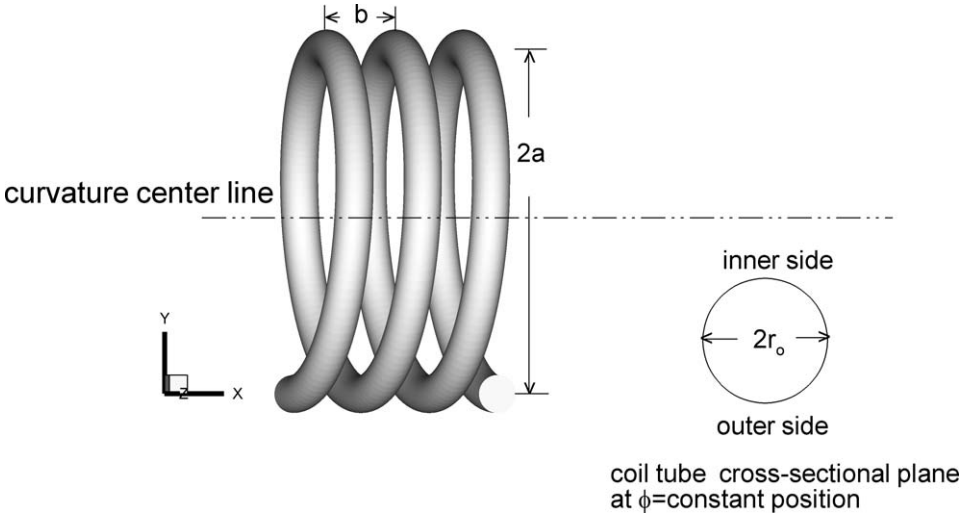

Fig. 1. Geometry of a helical coiled tube. Curvature ratio $\delta = r_0/a$.

parameters in the flow field of helical coiled tubes, including Reynolds number (Re), Nusselt number (Nu), Dean number (Dn) and Helical number (He). They are defined as follows:

$$Re = \rho V(2r_0)/\mu, \qquad Nu = \bar{h}(2r_0)/k$$
$$Dn = Re(r_0/a)^{1/2}, \qquad He = Dn/\left[1 + (b/2\pi a)^2\right]^{1/2}$$

where V and $\bar{h}$ are the average velocity and heat transfer coefficient in coiled tubes.

3. Entropy generation analysis

The present study focuses on steady, fully developed and laminar convection in helical coiled tubes with constant wall heat flux. The entropy generation analysis is similar to that derived by Bejan [9] for a straight pipe with circular cross section, and has been derived in the study of Ko and Ting [15]. The analysis is briefly described in the following.

Taking the coil passage of length dx as the thermodynamic system, the first and second law can be expressed as

$$\dot{m}\,\mathrm{d}h = q'\,\mathrm{d}x \tag{1}$$

$$\dot{S}'_{\mathrm{gen}} = \dot{m}\frac{\mathrm{d}s}{\mathrm{d}x} - \frac{q'}{T + \Delta T} \tag{2}$$

where $\dot{m}$, q' and $\dot{S}'_{\mathrm{gen}}$ are mass flow rate in coiled tubes, heat transfer rate and entropy generation rate per unit coil length, respectively. By using the thermodynamic relation

$$T\,\mathrm{d}s = \mathrm{d}h - v\,\mathrm{d}p \tag{3}$$

$\dot{S}'_{\mathrm{gen}}$ can be written as

$$\dot{S}'_{\mathrm{gen}} = \frac{q'\Delta T}{T^2(1 + \Delta T/T)} + \frac{\dot{m}}{T\rho}\left(-\frac{\mathrm{d}P}{\mathrm{d}x}\right) \tag{4}$$

Based on the relationship between friction factor f and pressure drop, and the heat transfer coefficient $\bar{h}$ and Nusselt number, $\dot{S}'_{\mathrm{gen}}$ can be expressed by

$$\dot{S}'_{\mathrm{gen}} = \frac{(q')^2}{T^2\pi\, Nu\, k + Tq'} + \frac{\dot{m}^3 f}{T\rho^2 r_0^5 \pi^2} \tag{5}$$

The only difference between the final form and the derivation of Bejan [10] is that the $\Delta T/T$ term in Eq. (4) has been retained in the present derivation for accuracy. The non-dimensional entropy generation number N_S [10] is defined as $\dot{S}'_{\mathrm{gen}}/(q'/T)$, and can be obtained from Eq. (5) as

$$N_S = (N_S)_T + (N_S)_P \tag{6}$$

where

$$(N_S)_T = \frac{1}{Nu\,\eta_1 + 1} \tag{7}$$

$$(N_S)_P = \frac{f\,Re^5}{\eta_2} \tag{8}$$

η_1 and η_2 are two dimensionless duty parameters, defined as

$$\eta_1 = \pi k T/q' \tag{9}$$

and

$$\eta_2 = 32\dot{m}^2\rho^2 q'/\mu^5\pi^3 \tag{10}$$

$(N_S)_T$ and $(N_S)_P$ represent the contribution of entropy generation from heat transfer irreversibility and fluid friction irreversibility, respectively.

For analyzing entropy generation, the information of f and Nu in helical coiled tubes is required in Eq. (6). The present study selected the correlations of f and Nu for fully developed laminar convection in helical coiled tubes with constant wall heat flux proposed by Manlapaz and Churchill [4]. The correlations are as follows:

$$f = \frac{16}{Re}\left[\left(1 - \frac{0.18}{[1 + (\frac{35}{He})^2]^{1/2}}\right)^m + \left(1 + \frac{r_0}{3a}\right)^2 \frac{He}{88.33}\right]^{1/2} \tag{11}$$

and

$$Nu = \left[\left(\frac{48}{11} + \frac{51/11}{(1 + \frac{1342}{Pr\,He^2})^2}\right)^3 + 1.816\left(\frac{He}{1 + \frac{1.15}{Pr}}\right)^{3/2}\right]^{1/3} \tag{12}$$

where values of m are 2, 1 and 0 for $Dn < 20$, $20 < Dn < 40$, and $Dn > 40$, respectively. Substituting the expressions of f and Nu into Eq. (6), N_S can be obtained as a function of Re, λ, δ, Pr, η_1 and η_2. Notably, the first and second terms of the right-hand side of Eq. (6), corresponding to the entropy generated by the irreversibility from heat transfer and fluid friction, respectively, may change with opposite signs. Thus, finding the optimal trade-off according to the entropy generation minimization principal becomes a critical challenge for heat exchanger designers.

4. Results and discussion

From the previous study of Ko and Ting [15], it is known that the influence of λ on N_S is relatively minor, therefore, the effect of λ is not necessary to be included. In the following analysis, λ is set as 0.05. Nonetheless, N_S is still a very complicated function of Re, δ, Pr, η_1 and η_2. It is very hard to determine the functional extreme by using calculus methods. In the present study, therefore, N_S is calculated directly through a multi-dimensional mapping that varies some parameter while holding others constant, and then the optimum case is found out based on the minimal entropy generation principle. The analysis range of Re is between 100 and 10 000. According to the research of Srinivasan [17], the critical Re for the helical pipe flow, which determines the flow is laminar or turbulent, is related to the curvature ratio as follows:

$$Re_{\text{crit}} = 2100\left(1 + 12\delta^{1/2}\right) \tag{13}$$

For ensuring the flow belongs to laminar regime, the smallest value of δ for a case with specified Re is calculated from Eq. (13). If the smallest value is less than 0.01, the starting value of δ would be 0.01. The upper limit of the analyzed δ is 0.3. Two working fluids, including air and water, are computed and analyzed.

4.1. Analysis of a baseline case: $\eta_1 = 2.41$ and $\eta_2/1.\text{E}20 = 0.05$; working fluid: air

A baseline case with $\eta_1 = 2.41$ and $\eta_2/1.0\text{E}20 = 0.05$, and using air as working fluid is analyzed first. Since friction factor and Nusselt number are closely related with the entropy generation in flow fields, the influence of δ on these two quantities is investigated based on the calculations according to the correlation equations, Eqs. (11) and (12), proposed by Manlapaz and Churchill [4]. Figs. 2 and 3 show the distributions of f and Nu with different δ and Re, respectively. The straight tube case is also included in the figures for comparison. From the figures, it can be found that f decreases and Nu increases as Re increases for all cases with different δ. Both of f and Nu increase with the increase of δ, which reveals the embarrassing situation that the increases of Nu to enhance heat transfer performance by increasing of δ will simultaneously cause the increase of friction loss. Such conflict effect induces the requirement of the optimal trade-off by selecting the most appropriate δ for the best exergy utilization and least irreversibility.

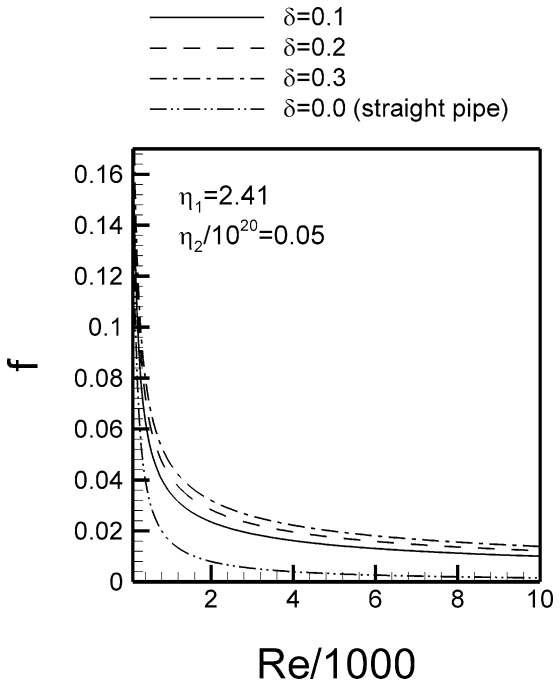

Fig. 2. Relationship between friction factor and Re and δ for the baseline case with $\eta_1 = 2.41$, and $\eta_2/1.\text{E}20 = 0.05$.

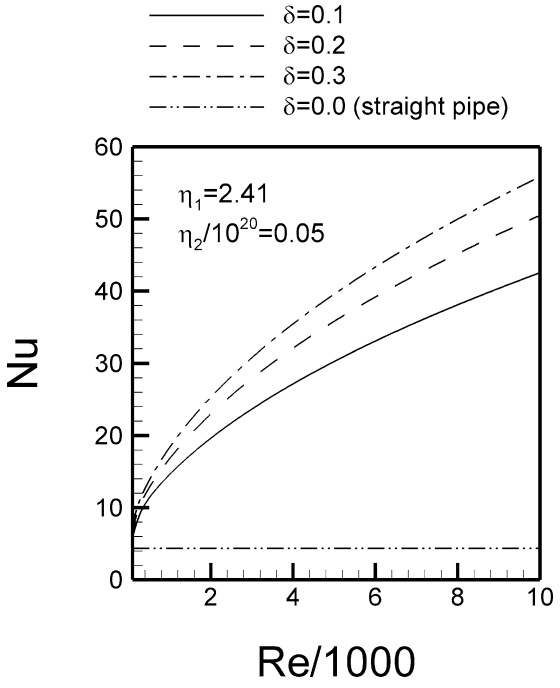

Fig. 3. Relationship between Nusselt number and Re and δ for the baseline case with $\eta_1 = 2.41$, and $\eta_2/1.\text{E}20 = 0.05$.

In order to understand the detailed contribution of entropy generation from frictional irreversibility and heat transfer irreversibility, investigations of the effects of δ on $(N_S)_P$ and $(N_S)_T$ have been carried out for the baseline case. Fig. 4 shows the influences of δ on $(N_S)_P$ and $(N_S)_T$ for cases with $Re =$ 1000, 3000, 5000 and 7000, respectively. The competition between the entropy generation from frictional irreversibility and heat transfer irreversibility can be seen very different in various

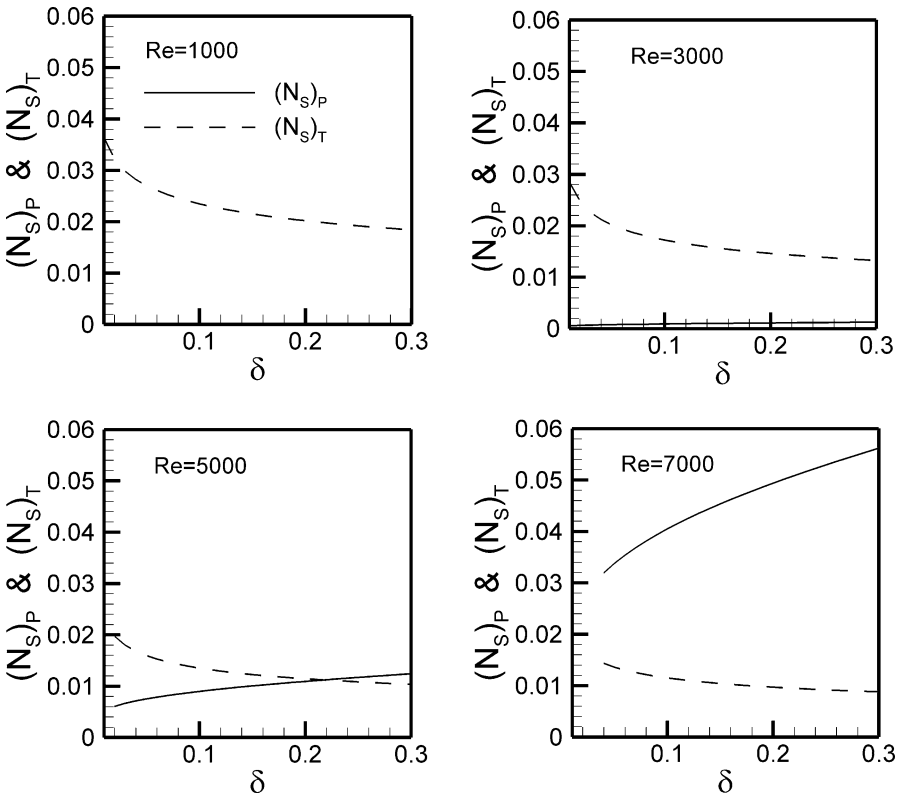

Fig. 4. The influence of δ on $(N_S)_T$ and $(N_S)_P$ of a baseline case with $\lambda = 0.05$, $\eta_1 = 2.41$, $\eta_2/1.E20 = 0.05$, and various *Re*.

Re cases. In $Re = 1000$ case, the values of $(N_S)_P$ are nearly zero, which indicates the major entropy generation comes from heat transfer irreversibility in the case. As *Re* increases to 3000, it can be seen that $(N_S)_P$ increases but $(N_S)_T$ decreases. However, $(N_S)_T$ is still much larger than $(N_S)_P$ for all δ cases, which implies the entropy generation is dominated by the heat transfer irreversibility under the *Re*. When *Re* further increases to 5000, the curves of $(N_S)_P$ and $(N_S)_T$ intersect at $\delta = 0.217$. When δ is larger than the intersected δ, $(N_S)_P$ is larger than $(N_S)_T$ and *vice verse* when δ is less than the intersected δ. In $Re = 7000$ case, $(N_S)_P$ increases significantly and turns out to be larger than $(N_S)_T$ for all δ cases, which indicates the entropy generation due to frictional irreversibility becomes the dominant source. Since heat transfer irreversibility dominates in lower *Re* regime, the changes of $(N_S)_T$ are more appreciable in lower *Re* cases. For the similar reason, the changes of $(N_S)_P$ are more appreciable in larger *Re* cases since frictional irreversibility dominates in larger *Re* regime. The above results shown in Fig. 4 clearly exhibit that the increase of *Re* can cause $(N_S)_P$ to increase and $(N_S)_T$ to decrease. Besides, the trend remains as the same for all δ cases. Such influences of *Re* on entropy generation could be understood from the effects of *Re* on fluid friction and heat transfer performance. As *Re* increases, the fluid friction in flow fields will increase, and thus results the increase of entropy generation due to friction irreversibility. On the contrary, the increase of *Re* will enhance the heat transfer performance, making the temperature gradient in flow fields become gentle, and in turn result the decrease of heat transfer irreversibility and entropy generation. The detailed investigation and discussion about the effects of *Re* on entropy generation and optimal *Re* with the minimal entropy generation can be found in the previous work of Ko and Ting [16]. The effects of δ, which is the major concern of the present paper, can also be observed from Fig. 4. In all of the four *Re* cases, it can be seen that $(N_S)_P$ increases and $(N_S)_T$ decreases as δ increases. The results come from that the increase of δ causes both of f and *Nu* to increase. The increase of f raises fluid friction and irreversibility, whereas the increase of *Nu* enhances the heat transfer performance and causes heat transfer irreversibility to reduce. It can also be found that the variation of $(N_S)_P$ with δ is found to become much steeper as *Re* increases, whereas the change of $(N_S)_T$ with δ is steeper in lower *Re* cases. The reason to induce the results is that $(N_S)_P$ is the dominant source in higher *Re* cases, therefore, the change of $(N_S)_P$ caused by the change of δ will be more significant in cases with higher *Re*. On the other hand, $(N_S)_T$ is the dominant entropy generation in lower *Re* cases, therefore, change of $(N_S)_T$ in lower *Re* cases is more apparent. The opposite influence of δ on the entropy generation from frictional and heat transfer irreversibility makes the optimal trade-off by selecting an optimal δ become an important issue.

Fig. 5 depicts the N_S vs δ plot for the baseline case, and *Re* as a parameter. Since the entropy generation in the lower *Re* ($Re = 1000$ and 3000) cases is dominated by heat transfer irreversibility, the change of N_S is mainly determined by $(N_S)_T$. As discussed previously, the increase of δ would enhance heat transfer performance, and in turn reduce the heat transfer irreversibility, therefore, N_S in these two cases with

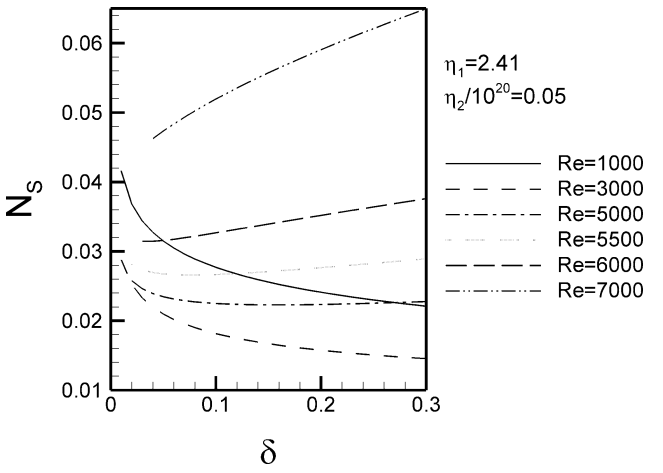

Fig. 5. The influence of δ on N_S of a baseline case with $\lambda = 0.05$, $\eta_1 = 2.41$, $\eta_2/1.E20 = 0.05$, and various Re.

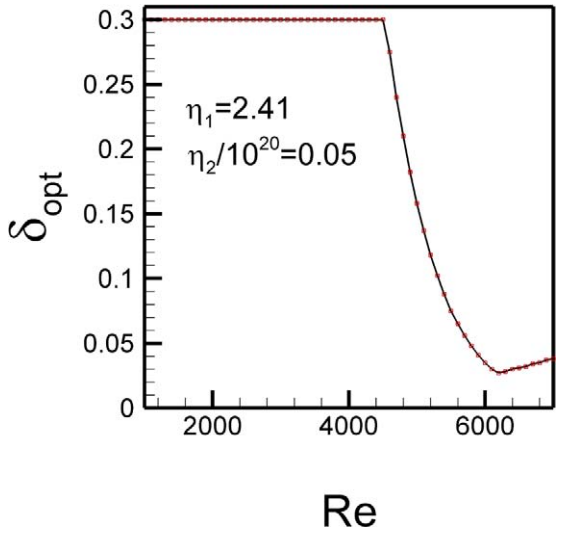

Fig. 6. Optimal δ for the baseline cases with $\lambda = 0.05$, $\eta_1 = 2.41$, and $\eta_2/1.E20 = 0.05$, and various Re.

lower Re can be seen to decrease monotonically with the increase of δ, i.e. the optimal δ for the two cases is the largest δ considered in the present study, 0.3. In addition, although the larger Re would simultaneously induce more serious fluid friction and enhance the heat transfer performance, it can be seen that N_S in $Re = 3000$ is lower than that in $Re = 1000$ case for all δ cases. This is resulted from that the entropy generation is dominated by heat transfer irreversibility in the two lower-Re cases, and the heat transfer performance is better in the larger Re case. As Re increases to 5000 and 5500, the competition between $(N_S)_P$ and $(N_S)_T$ becomes very complicated, and no one is really dominant in the flow field. The reversed influences of δ on $(N_S)_P$ and $(N_S)_T$ require the trade-off to determine the optimal δ with the minimal entropy generation. The optimal δ for the two cases can be seen to decrease with the increase of Re. Besides, when Re increases from 5000 to 5500, N_S increases for all δ cases. Such results come from that the frictional irreversibility becomes more dominant as Re increases, and the more serious entropy generation due to frictional irreversibility

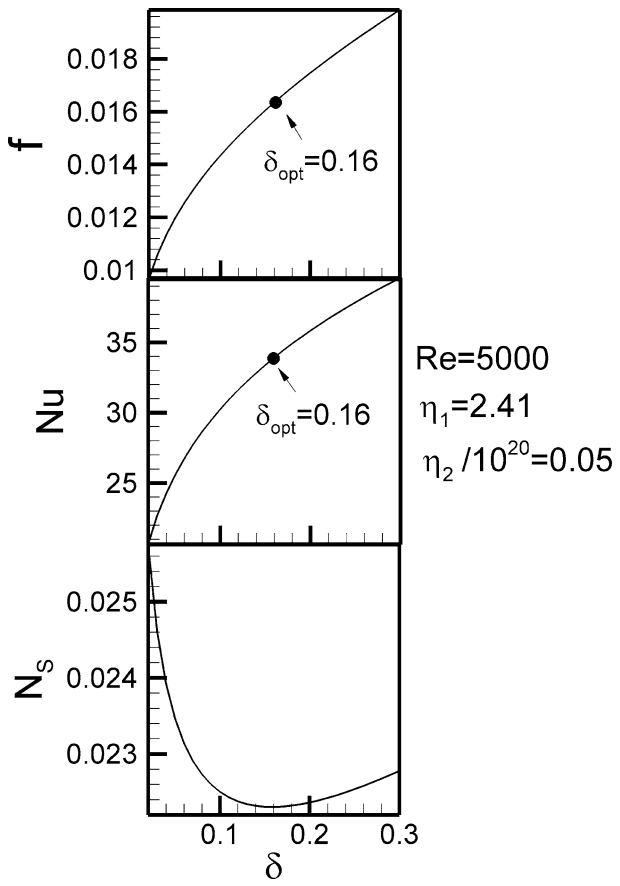

Fig. 7. Influences of δ on f, Nu and N_S for the baseline case with $Re = 5000$.

would be raised when Re increases. Although the heat transfer irreversibility would decrease simultaneously, its contribution is relatively minor in these cases, and therefore the resultant entropy generation is determined by frictional irreversibility. As Re further increases to 6000 and 7000, the entropy generation is totally dominated by fluid frictional irreversibility. It can be seen that N_S for the two cases increases monotonically with the increase of δ since the larger δ would cause more serious fluid friction. In these cases, the optimal δ is the smallest δ corresponding to the Re for ensuring the flow is laminar. The above observations of the relationship between the optimal δ and Re from Fig. 5 can be summarized as follows. When Re is low enough, the entropy generation is dominated by heat transfer irreversibility, therefore the larger δ should be used for minimal entropy generation since the larger δ can enhance heat transfer performance and reduce the heat transfer irreversibility. On the other hand, when Re is large enough, the entropy generation is dominated by frictional irreversibility; therefore the smaller δ should be used since the frictional irreversibility is smaller in the smaller δ cases. For cases with medium Re, the optimal δ is determined by an optimal trade-off since the entropy generation from frictional and heat transfer irreversibility compete with each other. Besides, the optimal δ decreases as the Re increases since the entropy generation from frictional irreversibility becomes more dominant as Re increases. Fig. 6 shows the relationship between optimal δ and Re for the baseline case, through which the above discussion is reflected. The

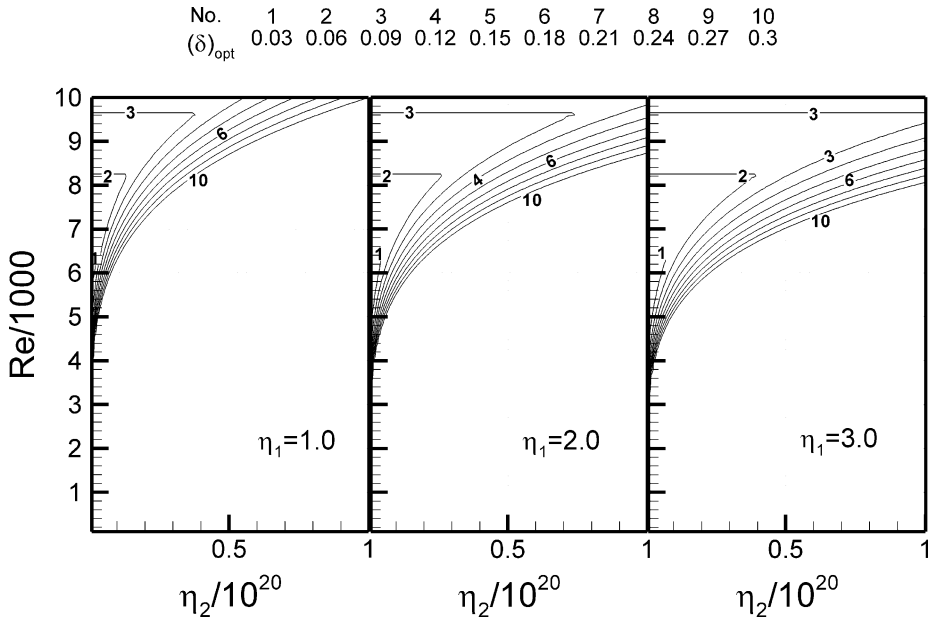

Fig. 8. Optimal δ contours on Re–η_2 plane for cases with $\eta_1 = 1$, 2 and 3.

figure is drawn from $Re = 1000$–7000 with the increment of 100. It can be seen that the relation between optimal δ and Re can be separated into three regions by two critical Re. In the first region, where Re is less than 4500, the optimal δ keeps the same for all Re as the largest δ considered in the present paper, i.e. 0.3. In the second range, where Re is larger than 4500 and less than 6200, the optimal δ decreases with the increase of Re. In the third range, where Re exceeds 6200, the optimal δ is the smallest δ corresponding to the Re for ensuring the flow is laminar, which mildly increases as Re increases.

For further investigating the friction and heat transfer performance under the optimal δ, Fig. 7 shows the influences of δ on f, Nu and N_S for the baseline case with $Re = 5000$. In the figures, f and Nu are based on the experimental correlation equations, Eqs. (11) and (12), whilst N_S is from the present analysis. The optimal δ with minimal N_S observed from the N_S–δ plot is 0.16. By using the optimal δ, it can be seen that f is not smallest and Nu is not largest, i.e. neither friction loss nor heat transfer performance is optimal. Nevertheless, from the view point of thermodynamic second law, the δ is best since the optimal trade-off between the entropy generation from frictional and heat transfer irreversibility is achieved at this value of δ.

4.2. Analysis of optimal δ for general flow conditions

In light of N_S being insensitive to λ, the optimal δ to yield the minimum entropy generation becomes a function of Re, η_1 and η_2. The above discussion has been focused on the baseline case with $\eta_1 = 2.41$ and $\eta_2/1.0\text{E}20 = 0.05$. In order to get the more general information about the optimal δ for different Re, η_1 and η_2 cases, further calculations were conducted for the cases with $\lambda = 0.05$, Re ranging from 100 to 10 000, η_1 from 0.1 to 3.0, and $\eta_2/1.0\text{E}20$ from 0.01 to 1.0. From the resultant distributions of N_S, the optimal δ for the cases with various combination of Re, η_1 and η_2 were deduced. Fig. 8 shows the optimal δ contours on the Re–η_2 plane with $\eta_1 = 1.0$, 2.0 and 3.0 cases, respectively. It can be seen from the figure that the optimal δ is sensitive to Re and η_2 in the upper left corners, and the region of the corner is found to become larger as η_1 increases. In the corner zone, the optimal δ increases as η_2 increases, and decreases as Re increases. Except the upper left corner region, the optimal δ keeps as the largest δ considered in present paper, 0.3. Figs. 9 and 10 show the relation between optimal δ and Re for $\eta_1 = 1.0$, 2.0 and 3.0; and $\eta_2/1.0\text{E}20 = 0.05$, 0.6 and 0.9 cases, respectively. The figures reveal the similar trend, that the relation between optimal δ and Re can be separated into three regions by two critical Re. In the first region, where Re is less than the first critical Re, the optimal δ keeps the same for all Re as the largest δ considered in the present paper, i.e. 0.3. In the second range, where Re is larger than the first critical Re and less than the second critical Re, the optimal δ decreases with the increase of Re. In the third range, where Re is larger than the second critical Re, the optimal δ increases as Re increases. The reason to cause such results has been explained in previous discussion according to the baseline case as shown in Fig. 5. Notably, the two critical Re is dependent on the values of η_1 and η_2.

4.3. Correlation equation for optimal δ for general flow conditions

Based on the observation from Figs. 9 and 10, the correlation between the optimal δ and Re, η_1 and η_2 are assumed as the following functional form:

$$\delta_{\text{opt}} = \begin{cases} 0.3 \quad \text{when } Re/1000 < f_1(\eta_1, \eta_2) \\ K_1 \eta_1^{A_1} (\eta_2/10^{20})^{B_1} (Re/1000)^{C_1} \\ \qquad \text{when } f_1(\eta_1, \eta_2) \leqslant Re/1000 < f_2(\eta_1, \eta_2) \\ K_2 \eta_1^{A_2} (\eta_2/10^{20})^{B_2} (Re/1000)^{C_2} \\ \qquad \text{when } Re/1000 \geqslant f_2(\eta_1, \eta_2) \end{cases} \quad (14)$$

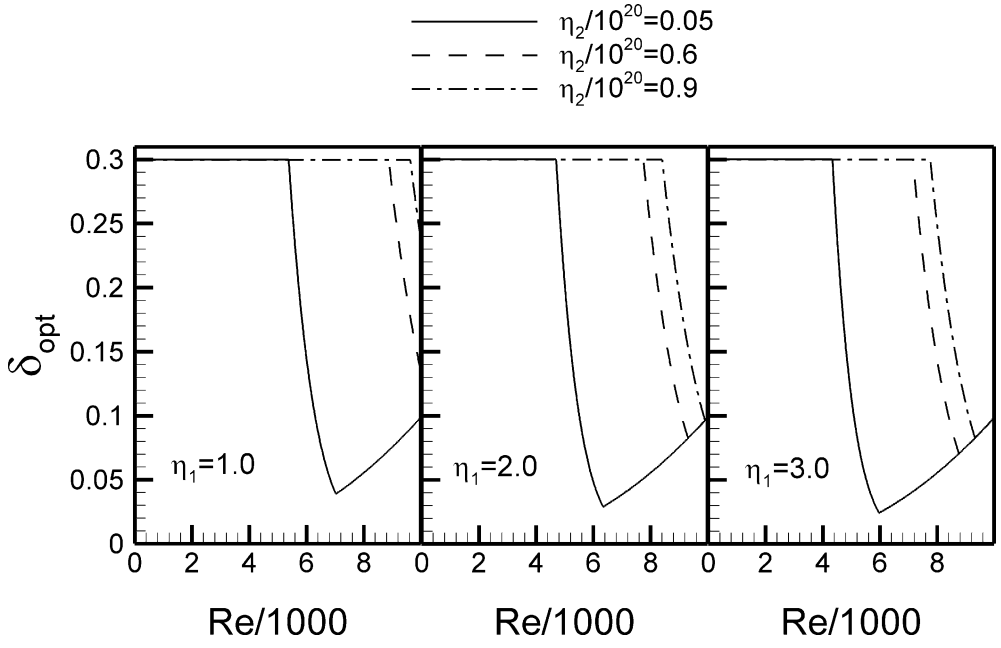

Fig. 9. Relationship between optimal δ and Re for cases with various values of η_1 and η_2.

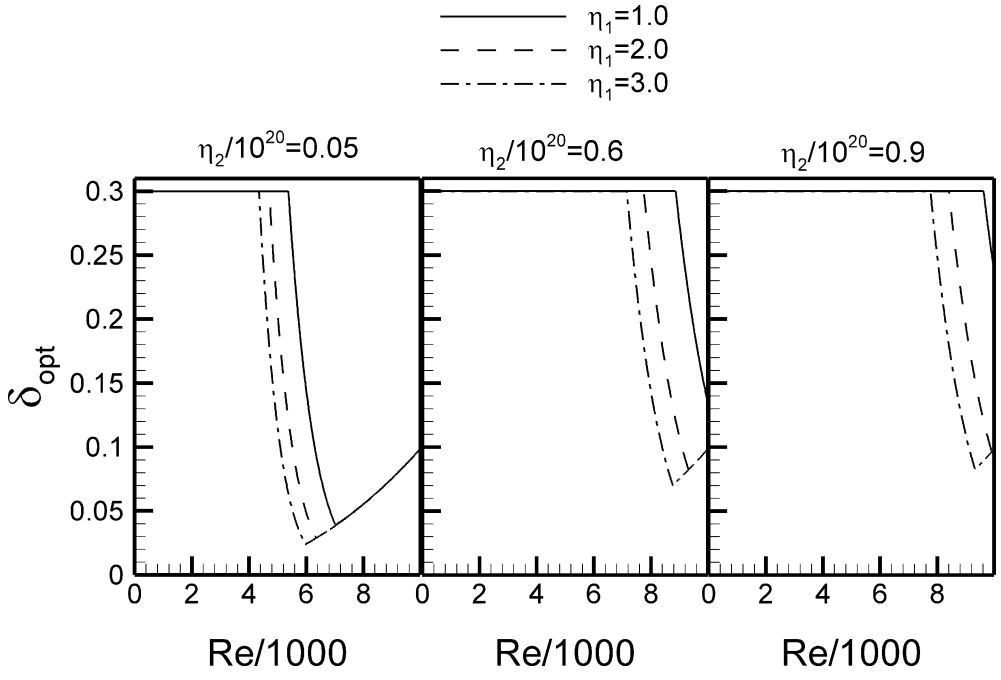

Fig. 10. Relationship between optimal δ and Re for cases with various values of η_1 and η_2.

From the calculated results, the functions $f_1(\eta_1, \eta_2)$ and $f_2(\eta_1, \eta_2)$ are first found out through the optimal analysis. Then, by using the least-square-error analysis, the correlation equation between δ_{opt} and Re, η_1 and η_2 can be obtained. The correlation equation of δ_{opt} for helical coiled tubes using air as working fluid is shown in Table 1. The average error of the correlation equation is 2.94% when $f_1(\eta_1, \eta_2) \leqslant Re/1000 < f_2(\eta_1, \eta_2)$, and 3.95% when $Re/1000 \geqslant f_2(\eta_1, \eta_2)$. The similar entropy generation analysis has also been carried out by using water as working fluid. The correlation equation of δ_{opt} is also shown in Table 1. The average error of the correlation equation is 2.99% when $f_1(\eta_1, \eta_2) \leqslant Re/1000 < f_2(\eta_1, \eta_2)$, and 1.57% when $Re/1000 \geqslant f_2(\eta_1, \eta_2)$.

It is noted that the design parameters, including Re, η_1 and η_2 are determined according to flow conditions in practical application, e.g. the mass flow rate of working fluid, the coiled tube size and the external wall heat flux. As these design parameters of helical coiled tubes are determined, the optimal δ can be calculated from the correlation equation provided in Table 1. The optimal δ should be adopted as the best flow configuration so that the thermal system of helical coiled tubes could have the best exergy utilization and least irreversibility.

Table 1
Optimal δ for helical coiled tubes for air and water as working fluid

Air		
$f_1(\eta_1,\eta_2) = 9.834\eta_1^{-0.197}(\eta_2/10^{20})^{0.202}$		
$f_2(\eta_1,\eta_2) = 10.633\eta_1^{-0.106}(\eta_2/10^{20})^{0.145}$		
Re	δ_{opt}	Average error
$Re/1000 < f_1(\eta_1,\eta_2)$	0.3	
$f_1(\eta_1,\eta_2) \leqslant Re/1000 < f_2(\eta_1,\eta_2)$	$8\,744\,591\eta_1^{-1.433}(\eta_2/10^{20})^{1.519}(Re/1000)^{-7.495}$	2.94%
$Re/1000 \geqslant f_2(\eta_1,\eta_2)$	$2.3635\times10^{-4}\eta_1^{-0.074}(\eta_2/10^{20})^{0.018}(Re/1000)^{2.664}$	3.95%
Water		
$f_1(\eta_1,\eta_2) = 9.109\eta_1^{-0.195}(\eta_2/10^{20})^{0.200}$		
$f_2(\eta_1,\eta_2) = 10.385\eta_1^{-0.136}(\eta_2/10^{20})^{0.148}$		
Re	δ_{opt}	Average error
$Re/1000 < f_1(\eta_1,\eta_2)$	0.3	
$f_1(\eta_1,\eta_2) \leqslant Re/1000 < f_2(\eta_1,\eta_2)$	$5\,284\,560\eta_1^{-1.446}(\eta_2/10^{20})^{1.517}(Re/1000)^{-7.516}$	2.99%
$Re/1000 \geqslant f_2(\eta_1,\eta_2)$	$1.472\times10^{-4}\eta_1^{-6.714/100\,000}(\eta_2/10^{20})^{-7.148/1000}(Re/1000)^{2.834}$	1.57%

Analysis range: η_1 from 0.1 to 3.0; η_2/1.0E20 from of 0.01 to 1.0; *Re* from 100 to 10000; δ from the lowest value calculated according to *Re* from Eq. (13) for ensuring laminar flow to 0.3.

5. Conclusion

In the present paper, the optimal δ for steady, laminar, fully developed forced convection in helical coiled tubes with constant wall heat flux is analyzed based on minimal entropy generation principle. Two working fluids, air and water, are considered. Through the entropy generation analysis for cases with *Re* from 100 to 10 000, η_1 from 0.1 to 3.0, η_2/1.0E20 from 0.01 to 1.0, the best correlation equation for the optimal δ as a function of *Re*, and is obtained by least-square-error analysis, and is presented in Table 1 for air and water as working fluid, respectively. The optimal δ is suggested to be adopted as the flow geometry for the helical coiled tubes so that thermal system can have the best exergy utilization and the least irreversibility.

References

[1] W.R. Dean, The stream-line motion of fluid in a curved pipe, Philos. Mag. Ser. 7 5 (30) (1928) 673–695.

[2] C.E. Kalb, J.D. Seader, Heat and mass transfer phenomena for viscous flow in curved circular tubes, Int. J. Heat Mass Transfer 15 (1972) 801–817.

[3] S.V. Patankar, V.S. Pratap, D.B. Spalding, Prediction of laminar flow and heat transfer in helically coiled pipes, J. Fluid Mech. 62 (1974) 539–551.

[4] R. Manlapaz, S.W. Churchill, Fully developed laminar convection from a helical coil, Chem. Engrg. Commun. 9 (1981) 185–200.

[5] S.A. Berger, L. Talbot, L.S. Yao, Flow in curved pipes, Annual Rev. Fluid Mech. 15 (1983) 461–512.

[6] R.K. Shah, S.D. Joshi, in: S. Kakac, R.K. Shah, W. Aung (Eds.), Handbook of Single-Phase Convective Heat Transfer, Wiley, New York, 1987 (Chapter 5).

[7] C.X. Lin, P. Zhang, M.A. Ebadian, Laminar forced convection in the entrance region of helical pipes, Int. J. Heat Mass Transfer 40 (14) (1997) 3293–3304.

[8] A. Narasimha, M. Sen, H.C. Chang, Heat transfer enhancement in coiled tubes by chaotic mixing, Int. J. Heat Mass Transfer 35 (10) (1992) 2475–2489.

[9] A. Bejan, Entropy Generation Minimization, CRC Press, Boca Raton, FL, 1996.

[10] A. Bejan, Entropy Generation Through Heat and Fluid Flow, Wiley, New York, 1982.

[11] P.K. Nag, N. Kumar, Second law optimization of convection heat transfer through a duct with constant heat flux, Int. J. Energy Res. 13 (1989) 537–543.

[12] A.Z. Sahin, Irreversibilities in various duct geometries with constant wall heat flux and laminar flow, Energy 23 (6) (1998) 465–473.

[13] A.Z. Sahin, Thermodynamics of laminar viscous flow through a duct subjected to constant heat flux, Energy 21 (12) (1996) 1179–1187.

[14] S.Z. Shuja, Optimal fin geometry based on exergoeconomic analysis for a pin-fin array with application to electronics cooling, Exergy 2 (2002) 248–258.

[15] T.H. Ko, K. Ting, Entropy generation and thermodynamic optimization of fully developed laminar convection in a helical coil, Int. Commun. Heat Mass Transfer 32 (2005) 214–223.

[16] T.H. Ko, K. Ting, Optimal Reynolds number for the fully developed laminar forced convection in a helical coiled tube, Energy Int. J., in press.

[17] P.S. Srinivasan, Pressure drop and heat transfer in coils, Chem. Engrg. (1968) 113–119.